Physica Scripta. Vol. T80, 133–140, 1999

QED Effects in Strong Nuclear Fields

I. Lindgren

Department of Physics, Chalmers University of Technology and Goteborg University, S-412 96 Goteborg, Sweden

Received September 14, 1998; revised version received October 8, 1998; accepted October 8, 1998

PACS ref: 31.30.Gs, Jv

Abstract

The present status of QED tests for heavy, highly charged ions with one or a few electrons is reviewed. The results of numerical calculations (to all orders in $Z\alpha$) of the Lamb shift for hydrogen-, helium- and lithiumlike ions are compared with recent experimental results. Also numerical calculations of the hyperfine structure and Zeeman effect in heavy hydrogenlike ions are discussed.

1. Introduction

1.1. *Early history of QED*

Quantum electrodynamics (QED) is the theory of interaction between particles—primarily electrons—and photons. The theory was introduced already in the late 1920's—shortly after the advent of quantum mechanics—by Dirac, Heisenberg, Pauli, Jordan and others [1]. The theory developed during the 1930's was quite successful in many respects, for instance concerning the spontaneous emission of radiation by atoms and much of the electromagnetic interaction between charged particles (scattering theory). Also the problem of *vacuum polarization*, i.e. the spontaneous creation and annihilation of electron-positron pairs in the vicinity of charged particles, was largely solved by Uehling in 1935 [2]. Particularly one problem remained unsolved during this decade, namely that of the particle *self energy* or the emission and subsequent reabsorption of photons by the same particle. The treatment of that processes lead to severe singularities that could not be handled. Many leading scientists at that time believed the problem was unsolvable. This skepticism hampered the development of QED for quite some time with the consequence that the solution was not found until a decade later [1].

In I. I. Rabi's atomic-beam laboratory at the Columbia university in New York three important experiments were carried out during the year of 1947 – experiments that turned out to be of fundamental importance for the scientific development. Nafe, Nelson and Rabi discovered a discrepancy between theory and experiment in the hyperfine structure of the hydrogen atom [3]. The observed discrepancy was much larger than the expected uncertainty in the theoretical evaluation. The experiment was reported at a famous conference on the Shelter Island outside Boston in June 1947 [1]. Shortly after the conference Gregory Breit suggested that the magnetic moment of the free electron may not be exactly one Bohr magneto—or that the g-factor was not exactly equal to 2, as predicted by the Dirac theory [4]. Such an anomaly could explain the Columbia experiment. This lead Polycarp Kusch and Henry Foley at the Rabi laboratory to investigate the g-factor of some simple atoms, where the valence electron can be regarded as essentially free [5]. They found an anomalous g-factor of $2 \times 1,00119$ (5), and with this value for the free electron the hyperfine structure of hydrogen could be perfectly explained. Early in 1948 Julian Schwinger [6] was able to report on a calculation of the electronic g-factor, using his newly developed relativistic QED. He found an anomalous g-factor of $2 \times (1 + \alpha/2\pi) = 2 \times 1,0011614\ldots$, in perfect agreement with the experimental result.

Also another very important experimental result was reported at the Shelter Island conference. Lamb and Retherford at the Columbia laboratory had determined the shift between the 2s and $2p_{1/2}$ levels in hydrogen, levels which should be exactly degenerate according to Dirac's theory [7]. This shift, now called the *Lamb shift*, was found to be about 1000 MHz. Directly after the conference Hans Bethe was able to derive a theoretical result for the shift, in almost perfect agreement with the experimental result, using non-relativistic QED. Shortly afterwards Schwinger as well as Richard Feynman and Sin-Itiro Tomanaga could arrive at essentially the same numerical result by means of the more rigorous covariant form of relativistic QED. In their work they showed that QED was exactly renormalizable to first order. In 1949 Freeman Dyson extended this proof to all orders of perturbation theory. This can be regarded as the birth of modern QED [1].

1.2. *Present status of QED*

In quantum electrodynamics the interaction with the electromagnetic field is treated perturbatively with the fine-structure constant α as the expansion parameter. For light systems, the standard theoretical technique is to treat also the nuclear field as a perturbation—with $Z\alpha$ as the expansion parameter—starting from plane-wave solutions of the Schrödinger or the Dirac equation. This technique is now well tested for systems like the neutral hydrogen and helium atoms, as well as for exotic systems like positronium and muonium. Remarkable agreement between theory and experiments has been achieved for the hyperfine structure and the Lamb shift of such systems and, in particular, also for the electronic and muonic g-factors. In some cases up to eighths order of perturbation theory has been applied in these calculations. Trusting that the theory is correct to that degree, the most accurate values for the fine-structure constant α can now be obtained by comparing experimental data of this kind with corresponding QED results [8].

In recent years considerable progress has been made—experimentally as well as theoretically—also in the study of highly charged few-electron systems. For such systems, where $Z\alpha$ approaches unity, it is no longer meaningful to treat the nuclear field perturbatively. Instead, the calculations have to be performed *non perturbatively*, taking *all orders* of $Z\alpha$ into account. This can be achieved by starting

from electronic states generated in the field of the nucleus (and possibly closed electronic shells), rather than free-electron states. Here, comparison between experimental and theoretical results will make it possible, for the first time, to perform accurate tests of QED independent of the $Z\alpha$ expansion. For such heavy systems the QED effects are much more pronounced. The Lamb shift in the ground state of hydrogenlike uranium, for instance [9], is about 470 eV (including a nuclear-size effect of about 200 eV) with an experimental uncertainty of about 13 eV. This could be compared to the corresponding shift in neutral hydrogen of 4 μeV. If the experimental accuracy could be somewhat improved, which is anticipated, the Lamb shift of highly charged hydrogenlike ions could constitute important test objects for strong-field QED.

Also heavy ions with more than one electron can be important objects for testing the QED at strong fields. The splitting between the $2p_{1/2}$ and 2s states in Li-like uranium has been measured by Schweppe *et al.* [10a] to be 280.59 eV with an uncertainty of only 0.09 eV. To a large extent this experiment formed the starting point for several theoretical groups to develop computational techniques for dealing with QED effects also in non-Coulombic potentials. Accurate experimental data are now available also for the $2s - 2p_{3/2}$ transition in Li-like uranium as well as for the $2s - 2p$ transitions in other Li-like ions [10b, c].

At Livermore Marrs *et al.* [11] have measured the binding energies of some He-like ions, and by comparing with the corresponding data for H-like ions the two-electron contribution to the level shift can be extracted. These data can be used for direct test of the *screening* of the first-order Lamb shift.

Also the hyperfine structure can now be measured with high accuracy for heavy H-like ions [12], and experiments of the Zeeman effect (g-factor) of such ions are in progress [13]. Such data will serve as important complement to the level-shift data for testing strong-field QED.

In the present talk the present status of QED calculations on highly charged ions will be reviewed. Numerical results will be given for different systems with one, two and three electrons and comparisons made with experimental results, when available. The possibility of making relevant tests of QED in strong nuclear fields will be discussed.

2 QED of single-electron systems

2.1. *First-order Lamb shift*

The first-order Lamb shift is caused by the effects represented by the two diagrams in Fig. 1, the *electron self-energy* and the *vacuum polarization*. The first-order self energy can be expressed by the second-order-S-matrix

$$S^{(2} = -e^2 \int\int \mathrm{d}^4x_1\, \mathrm{d}^4x_2\, T[(\Psi^\dagger \alpha^\nu A_\nu \Psi)_2 (\Psi^\dagger \alpha^\mu A_\mu \Psi)_1], \qquad (2.1)$$

where T represents the Wick time-ordering operator, Ψ, $\Psi^\dagger$ the field operators, A_μ the electromagnetic field and α^μ the Dirac operator in covariant form (related to the gamma matrices by $\alpha^\mu = \beta\gamma^\mu$). We use here the Furry interaction picture with the field operators expressed in terms of electron orbitals, generated in the field, U, of the atomic nucleus,

$$\begin{aligned} &\Psi = \sum a_i \phi \text{ and } \Psi^\dagger = \sum a_i^\dagger \phi_i^\dagger, \\ &h_\mathrm{D}\phi_i = \epsilon_i \phi_i;\ h_\mathrm{D} = \alpha \cdot p + \beta m + U. \end{aligned} \qquad (2.2)$$

$a_i^\dagger$ and a_i are creation and destruction operators, respectively. (Throughout the paper we will use relativistic units, $\hbar = m = c = \epsilon_0 = 1$ and $e^2 = 4\pi\alpha$, α being the fine-structure constant, but we will for clarity normally keep e in the equations.) The external-field orbitals are in the Feynman diagrams represented by *double lines*.

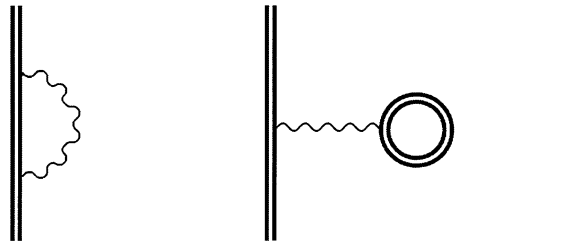

Fig. 1. The Feynman diagrams for the first-order Lamb shift of a bound electronic state. The first diagram represents the electron self energy and the second diagram the vacuum polarization.

Integration over the time coordinates yields the Feynman amplitude in the mixed energy-space representation

$$\begin{aligned} M = \int\int \mathrm{d}^3x_1\, \mathrm{d}^3x_2 \phi_a^\dagger(x_2) \mathrm{i}e\alpha^\nu \int \frac{\mathrm{d}\omega}{2\pi}\, \mathrm{i}S_F(x_2, x_1, \varepsilon_a - \omega) \\ \times \mathrm{i}e\alpha^\mu \phi_a(x_1) \mathrm{i}D_{F\nu\mu}(x_2 - x_1, \omega). \end{aligned} \qquad (2.3)$$

The electron propagator is given by

$$S_F(x_2, x_1, \omega) = \sum_i \frac{\phi_i(x_2)\phi_i^\dagger(x_1)}{\omega - \epsilon_i(1 - \mathrm{i}\eta)}, \qquad (2.4)$$

where the sum runs over the complete spectrum of single-electron states, with positive as well as negative energy (positron states). The photon propagator is in the Feynman gauge

$$D_{F\nu\mu}(x_2 - x_1, \omega) = -g_{\nu\mu} \int \frac{\mathrm{d}^3k}{(2\pi)^3} \frac{\mathrm{e}^{\mathrm{i}k\cdot(x_2 - x_1)}}{\omega^2 - k^2 + \mathrm{i}\eta}. \qquad (2.5)$$

This leads to the first-order bound-state self energy

$$\Delta E_\mathrm{bau} = e^2 \sum_t \left\langle at \left| (1 - \alpha_1 \cdot \alpha_2) \int \frac{\mathrm{d}^3k}{(2\pi)^3} \frac{\mathrm{e}^{\mathrm{i}k\cdot(x_2 - x_1)}}{\epsilon_a - \epsilon_t - k\,\mathrm{sign}(\epsilon_t)} \right| ta \right\rangle. \qquad (2.6)$$

For the numerical evaluation of an expression of the type (2.6), an expansion in spherical waves is normally used together with a "complete" spectrum of radial single-electron functions, the latter generated by solving the Dirac equation, using numerical basis set of spline [14] or space discretization type [15]. The expression is infinite, and in order to extract the physical result it has to be *renormalized*.

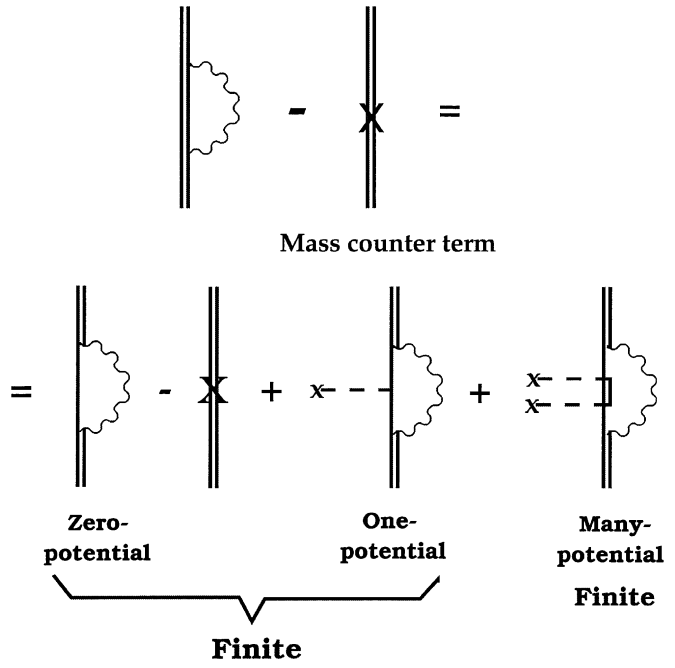

Fig. 2. Mass-renormalization of the first-order bound-state self energy and potential expansion of the bound-state propagator inside the self energy operator. The unrenormalized self energy as well as the mass counter term are infinite, but the infinities of the latter together with the zero- and one-potential terms cancel.

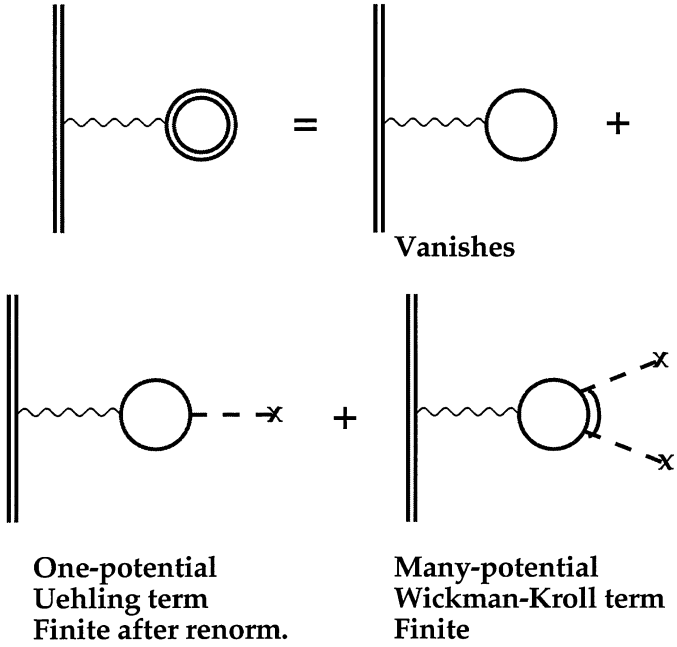

Fig. 3. Potential expansion of the first-order bound-state vacuum polarization. The zero-potential term vanishes identically. The one-potential term is infinite, but becomes finite after charge renormalization, leading to the so-called Uehling term.

For a free electron the self energy constitutes a part of the "physical" electron mass. This part is also present in the bound-state energy and has to be removed (the "*mass counter term*"), before the physically significant effect can be extracted. This is the *mass renormalization*. In order to handle the infinities, it is convenient to expand the external-field orbitals in terms of potential perturbations on electron orbitals, as illustrated in Fig. 2. The infinities of the zero- and one-potential terms together with the mass

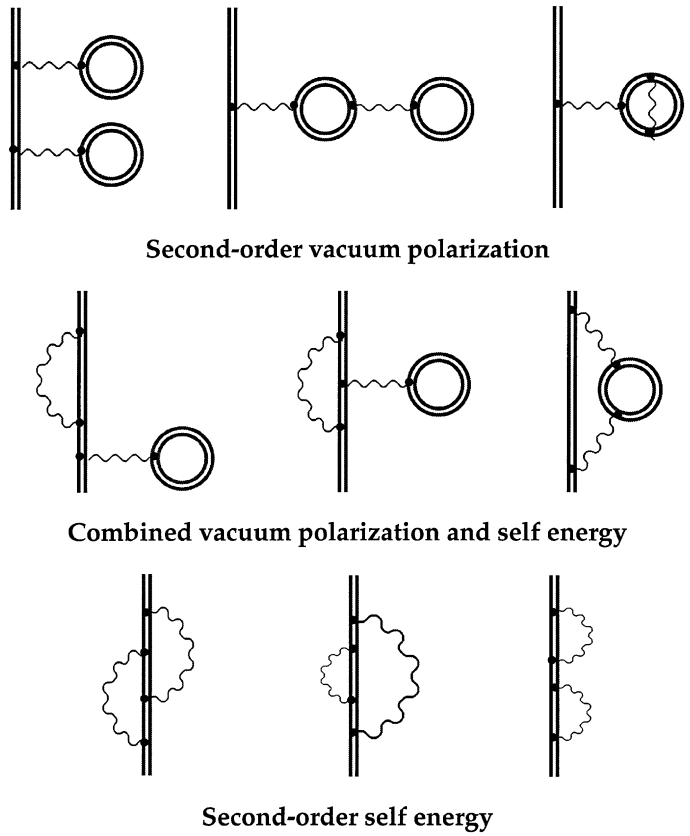

Fig. 4. Feynman diagrams for the second-order Lamb shift for one-electron systems.

counter term cancel. These parts can be handled analytically in the momentum representation. The last, many-potential term is finite and is evaluated numerically in the coordinate space.

Accurate non-perturbative calculations of the first-order self energy for hydrogenlike systems were first obtained by Peter Mohr and more recently by Mohr and Soff [16].

The first-order *vacuum polarization* can similarly be expanded using potential interactions, as illustrated in Fig. 3. The zero-potential term vanishes. The one-potential term is infinite but can after renormalization be expressed in a simple fashion by means of the *Uehling potential*, derived by Uehling already in 1935 [2]. The many-potential term, representing the so-called Wickman-Kroll effect [17], is finite and can be evaluated numerically with high accuracy, as shown by Mohr and Soff [18] and Persson *et al.* [19].

2.2. *Second-order Lamb shift*

For highly charged ions there is a realistic possibility to observe also effects beyond the first-order QED, i.e. two-photon effects, and this would constitute an additional important test of strong-field QED. For the Lamb shift the second-order self energy and vacuum-polarization Feynman diagrams are shown in Fig. 4.

The second-order vacuum polarization (first line) as well as the combined vacuum-polarization-self energy contributions (second line) have now been evaluated, including the Wickman-Kroll contribution [20]. The second-order self energy part (third line) has so far been only partially calculated [21].

Table I *Lamb shift of 1s level in H-like Uranium (in eV).*

	1s	Ref.
Finite nuclear size	198.68 (32)	
First-order QED		
(emm)Self energy	355.05	[16]
Vacuum polarization	−88.60	[19]
Nucl size + first-order QED	465.27 (32)	
Second-order QED		
Second-order vacuum pol	−0.94 (10)	[20]
Comb self-energy-vac pol.	1.27 (10)	[20]
Second-order self energy	±2	only partly calculated [21]
Second-order QED (calculated so far)	0.33 (2, 0)	
Nuclear polarization	−0.18	[22a]
Nuclear recoil	0.16*	[22b]
TOTAL THEORY	465.5 (2.0)	
EXPERIMENTAL	470 (16)	[9a]
	468 (13)	[9b]

*A value 0.145 eV was presented at the Bensheim conference Sept. 1998 by Yamanaka and Ichimura.

Table II. *The* $2_{p1/2} - 2s_{1/2}$ *transition in Li-like Uranium (in eV)*

	Lindgren *et al.* [24]	Blundell [23].
Relativistic MBPT	322.33 (2)	322/41
First-order QED		
Self energy	−54.32(15)	−54.24
Vacuum polarization	12.55 (4)	12.56
First-order QED Total	−41.77 (15)	−41.68
Second-order QED		
Second-order vacuum pol	0.13	
Combined self energy-vac pol.	−0.21	
Second-order self energy	NOT CALCULATED	
Second-order QED (calculated so far)	−0.08	
Nuclear polarization	0.03	0.03
Nuclear recoil	−0.08	−0.08
TOTAL THEORY	280.43 (25)	280.68 (10)
EXPERIMENTAL	280.59 (9)	

The 1s Lamb shift has been measured for some hydrogenlike systems with good accuracy at SIS/ESR at GSI [9]. This shift is normally defined as the difference between the experimental binding energy and thcorresponding Dirac value for a point nucleus. In Table I we show the experimental and theoretical results for hydrogenlike uranium ($Z = 92$). The agreement is quite good, and the theoretical result falls well within the experimental error limit of ±13 eV. The second-order contributions, which are not yet fully calculated, can be expected to be of the order of one or a few eV. This means that the experimental accuracy has to be improved one order of magnitude before this part can be tested. It should also be noted that the finite-nuclear-size effect, which is a part of the experimentally determined Lamb shift, is of the order 200 eV or half the total effect. This part can be calculated rather accurately, since the size and shape of the uranium nucleus is well know. The nuclear uncertainty can probably be further reduced by studying some nucleus with even better known properties, like ^{208}Pb. Nevertheless, the uncertainty in the finite-size effect will most likely always limit the possibilities of making accurate QED tests beyond first order for this type of systems.

2.3. *Single-electron in non-Coulombic potential*

An alkali atom, with a single electron outside closed electron shells, can to a large extent be treated as a system with a single electron, moving in the *non-Coulombic* field of the nucleus and the closed electron shells. The Lamb shift of the $n = 2$ state, or the $2p_{1/2} - 2s_{1/2}$ transition, of lithiumlike uranium was measured very accurately a few years ago by Schweppe *et al.* at the Bevalac at Berkeley [10]. This stimulated several groups to develop numerical methods for accurate QED calculations in the extended Furry interaction picture with non-Coulombic orbitals [23–25]. In this picture the electronic states are generated in the field of the nucleus *and* the closed electron shells (2.2). In Table II we show the experimental result compared with the theoretical results of Lindgren *et al.* [24a] and Blundell [23]. In addition to the QED contribution, it is here necessary to evaluate also the many-body contribution quite accurately, using the method described in the next section. The agreement between the experimental and theoretical results is here extremely good, of the order of a few tenths of a percent. This represents a good test of the numerical method for calculating the first-order Lamb shift in an arbitrary central field.

In the calculations of Lindgren *et al.* and Blundell, the effect of the interelectronic interaction (screening) on the Lamb shift is treated only approximately by modifying the single-electron potential.

A more exact calculation of that effect has recently been performed by Yerokhin *et al.* [24b]. The difference from the values of Lindgren *et al.* is only of the order of 0.01 eV.

Recently the $2s_{1/2} - 2p_{3/2}$ transition in Li-like bismuth has been measured with very high accuracy, ±0.039 eV, by Beiersdorfer *et al.*, using the Super-EBIT facility at Livermore together with a crystal spectrometer [10b]. The agreement with theoretical calculations is here as good as for the $2s_{1/2} - 2p_{3/2}$ transition in uranium.

As for the H-like ions discussed above, the second-order contributions are not fully calculated for the Li-like ions. However, these effects might very well be quite significant in the Li case, also with the present level of experimental accuracy. Therefore, it would be of great interest to get access to complete second-order results in this case in order to see if the good agreement still remains or if it is only fortuitous.

3. QED of many-electron systems

3.1. *Relativistic many-body perturbation*

For relativistic many-body perturbation theory (RMBPT) it might seem natural to start from the hamiltonian

$$H = \sum h_{\mathrm{D}} + \sum V_{ij}, \tag{3.1}$$

where h_{D} is the single-electron Dirac hamiltonian

$$h_{\mathrm{D}} = \alpha \cdot p + \beta m - \frac{e^2 Z}{4\pi r} \tag{3.1}$$

α and β being the Dirac operators and V_{ij} is the interelectronic interaction. (As before, we use relativistic units, $\hbar = m = c = \epsilon_0 = 1$ and $e^2 = 4\pi\alpha$). Although this hamiltonian has been used in many calculations, it suffers from

two serious problems. Firstly, the eigenvalues have no lower bound, due to the existence of the negative-energy solutions to the Dirac equation (Brown-Ravenhall disease [26]), and secondly the interelectronic potential V_{ij} is not uniquely determined (gauge dependent).

The first problem can be eliminated by introducing *projection operators*, Λ_+ [27]

$$H = \Lambda_+ \left[\sum_i h_{\mathrm{D}}(i) + \sum_{i<j} V_{ij} \right] \Lambda_+, \tag{3.3}$$

eliminating the negative-energy states. This is the *No-Virtual-Pair Approximation* (NVPA), which is a sound starting point for RMBPT. It remains to determine the interelectronic potential V_{ij}, which can be done by means of QED.

3.2. *The electron-electron interaction*

In QED the interaction between the electrons is represented by the exchange of virtual photons, as illustrated in Fig. 5(a). The second-order S-matrix for the single-photon exchange is after integration over the time given by

$$\begin{aligned} \langle cd|S^{(2)}|ab\rangle = &-2\pi \mathrm{i}\delta(\epsilon_a + \epsilon_b - \epsilon_c - \epsilon_d) \\ &\times \langle cd|\alpha_1^\mu \alpha_2^\nu e^2 D_{F\nu\mu}(x_2 - x_1, \omega_{ac})|ab\rangle. \end{aligned} \tag{3.4}$$

$D_{F\nu\mu}(x_2 - x_1, \omega_{ac})$ is as before the photon propagator and $\omega_{ac} = \epsilon_a - \epsilon_c$ the energy parameter. The delta factor demonstrates that energy is conserved at the interaction. The expression above can be compared with the S-matrix of *potential scattering*, represented by the Feynman diagram (b) in Fig. 5. This yields an effective *interaction potential*

$$V_{\mathrm{eff}}(\omega) = \alpha_1^\mu \alpha_2^\nu e^2 D_{F\nu\mu}(x_2 - x_1, \omega). \tag{3.5}$$

This potential is *energy-dependent* as well as *gauge dependent*, due to the appearance of the photon propagator.

In the Feynman and Coulomb gauges the interaction becomes in the *unretarded* (frequency independent) *limit*

$$V_{\mathrm{eff}}^{\mathrm{F}}(\omega \Rightarrow 0) = \frac{e^2}{4\pi r_{12}} (1 - \alpha_1 \cdot \alpha_2) \tag{3.6a}$$

$$V_{\mathrm{eff}}^{\mathrm{C}}(\omega \Rightarrow 0) = \frac{e^2}{4\pi r_{12}} \left(1 - \frac{1}{2} \alpha_1 \cdot \alpha_2 - \frac{(\alpha_1 \cdot r_{12})(\alpha_2 \cdot r_{12})}{2r_{12}^2} \right), \tag{3.6b}$$

respectively. Here, the first part represents the (instantaneous) Coulomb interaction and the remaining parts the *Gaunt* (3.6a) and the *Breit interactions* (3.6b), respectively.

The one-photon potentials obtained with the Feynman and Coulomb gauges give significantly different results when applied in iterative schemes, such as multi-configuration Dirac-Fock (MCDF) or RMBPT, but it can be shown that the Coulomb gauge yields the most accurate results (at least for light and medium-heavy atoms) [28]. This holds also when the unretarded interaction is used, and therefore this constitutes a good approximation for RMBPT. This leads to the

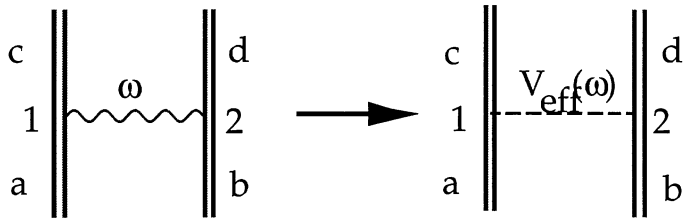

Fig. 5. The Feynman diagram for single-photon exchange (a) is compared with that of potential scattering (b).

No-Virtual-Pair Approximation with the Dirac-Coulomb-Breit hamiltonian

$$H = \Lambda_+ \left[\sum h_{\mathrm{D}} + \sum \left(\frac{e^2}{4\pi r_{ij}} + B_{ij}^0 \right) \right] \Lambda_+ \tag{3.7a}$$

where

$$B_{12}^0 = -\frac{e^2}{4\pi} \left(\frac{\alpha_1 \cdot \alpha_2}{2r_{12}} + \frac{(\alpha_1 \cdot r_{12})(\alpha_2 \cdot r_{12})}{2r_{12}^3} \right) \tag{3.7b}$$

is the unretarded Breit interaction. Many-body calculations based on the Dirac-Coulomb-Breit Hamiltonian will form the starting point for our analysis of systems with more than one electron. Effects beyond that approximation are defined as "*Many-Body QED-effects*". *These are of two kinds, non-radiative effects* (due to retardation and negative-energy states) and *radiative effects* (self energy and vacuum polarization). The radiative effects lead as for single-electron systems to the *Lamb shift*.

3.3. *QED of two-electron systems*

Recently, the two-electron contribution to the binding energy of the ground state of some He-like ions has been measured at the Super-EBIT facility at Livermore by Marrs *et al.* [11]. In this experiment the binding energies of He- and H-like ions of the same element have been compared, which makes it possible to eliminate very accurately all single-particle effects and to extract the pure two-particle contribution. In this way, most of the nuclear effect as well as the single-electron Lamb shift is eliminated. The remaining two-electron effect in second order is represented by the diagrams in Fig. 6. The first line represents the non-radiative QED effects, discussed above and calculated by Blundell *et al.* [29b] as well as by Lindgren *et al.* [29a]. The second and third lines represent he radiative effects (Lamb shift), and the first complete QED calculation to second order was first performed by Persson *et al.* [29a]. The results are compared with the corresponding experimental results in Table III. More recently, a numerically more accurate calculation of the two-electron Lamb-shift diagrams (lines 2 and 3 in Fig. 6) has been performed by Yerokhin *et al.* [29c]. The corresponding total results are also given in Table III, and the agreement between the two theoretical calculations is found to be extremely good.

The agreement between the theory and experiment is also quite good in this case, although the experimental accuracy is not yet sufficient for testing the many-body QED contributions. However, only a moderate increase of the accuracy is needed for this purpose. The uncertainty due to the finite nuclear size is very small in this case, and therefore these sys-

Table III *Two-electron contribution to the ground-state energy of He-like ions. Comparison between theory and experiment (in eV)*

Nuclear charge	M B P T			Non-radiative	Lamb shift	Total theory		Experimental
	First order	2nd	3rd			[29a]	[29b]	Marrs *et al.* [11]
32	567.61	−5.22	0.02	0.03	−0.42	562.02 (10)	562.02 (1)	562.22 ± 1.6
54	1036.56	−7.04	0.03	0.16	−1.56	1028.15 (10)	1028.15 (10)	1027.2 ± 3.5
66	1347.45 (1)	−8.59	0.03	0.36	−2.66	1336.59 (10)	1336.58 (4)	1341 ± 4.3
74	1586.93 (2)	−9.91	0.04	0.55	−3.68	1573.93 (10)	1573.92 (6)	1568.9 ± 15
83	1897.56 (4)	−11.77	0.04	0.86	−.5.16	1881.1 (2)	1881.50 (7)	1876 ± 14
92	2265.87 (10)	−14.16	0.05	1.28	−7.12	2245.9 (2)	2245.92 (9)	

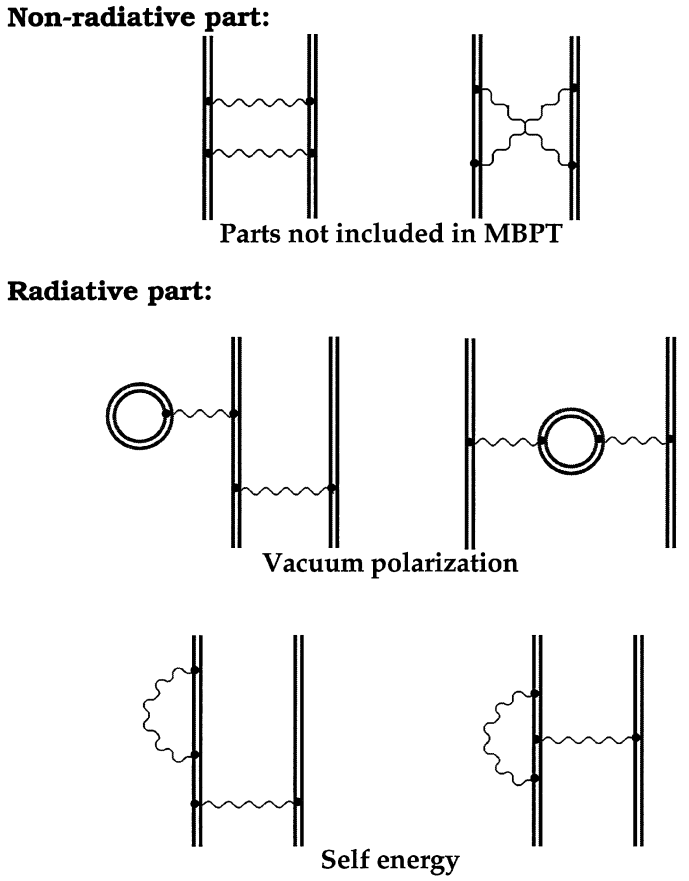

Fig. 6. Feynman diagrams for the second order contribution to the two-electron part of the binding energy of He-like systems. The first line represents the many-body part as well as the non-radiative QED part, not present in relativistic MBPT. The remaining lines represent the radiative contribution (screening of the Lamb shift).

tems might constitute very good objects for testing second-order QED effects at strong fields.

There exist also very accurate experimental data of the separations between *excited states* of He-like ions, particularly in the light and medium-heavy region. Calculations of the two-electron QED effects are now under way at several places. When these results become available, more extensive tests of the two-electron QED effects can be performed.

4. Hyperfine structure and Zeeman effect

4.1. *The hyperfine structure*

The hyperfine structure of the ground state of several highly charged H-like ions has now been measured with high accuracy. Here, we shall in particular consider the bismuth ion for which experimental result is obtained at GSI by Klaft *et al.* [12]. A corresponding numerical calculation has been performed by Persson *et al.* [30] and more recently by Blundell *et al.* [31]. The results obtained by Persson *et al.* are compared with the experimental result in Table IV. (The theoretical result of Blundell *et al.* is about 1% larger than those of Persson *et al.*). The main uncertainty of the theoretical evaluation is due to the experimental nuclear magnetic moment, which is based on an old nmr measurement, and thus subject to a significant and largely unknown chemical shift. Another large uncertainty is associated with the effect of the magnetic distribution inside the nucleus (the Bohr-Weisskopf effect). This is here taken from a recent estimate by Shabaev *et al.* [32]. The uncertainty due to the nuclear charge distribution is considerably smaller.

Table IV *Hyperfine structure in H-like Bi (in eV) [30].*

Point-nucleus value	5.825*
Finite nuclear size**	
Charge distribution	−0.634 (1)
Magnetic distribution (Bohr-Weisskopf)	−0.061 (18)
Non-QED value	5.130 (18)
First-order QED corrections	
Self energy	−0.059
Vacuum polarization	0.030
Sum QED corrections	−0,030
TOTAL THEORY	5.100 (20)
EXPERIMENTAL	5.084 (1) [12]

*Based on magnetic moment of 4,1106 nuclear magnetons. Uncertainty not considered.
**Based on nuclear rms 5.519 fm.

For lighter elements the QED effect on the hyperfine structure can be expressed as a power expansion in a and $Z\alpha$. For single-photon processes, the result is conventionally expressed in the form

$$\Delta E^{\mathrm{hfs}} = \Delta E^{(1)}\left(1 + \frac{\alpha}{2\pi} + \cdots\right) = \Delta E^{(1)}\left(1 + \frac{\alpha}{\pi} F(Z\alpha)\right).$$

where $\Delta E^{(1)}$ is the first-order splitting and $F(Z\alpha)$ is a general function of $Z\alpha$, representing the radiative effects. The coefficients for the quadratic and cubic terms of $F(Z\alpha)$ have recently been obtained by Pachucki [33] and Karshenboim [34]. In Fig. 7 these approximations are compared with the all-order numerical result. There it can be seen that the quadratic form can be used with reasonable accuracy up to $Z = 15$ à 20 and the cubic form to $Z = 30$ à 40. For much higher Z values it is obvious that the convergence of the $Z\alpha$ expansion will be very slow.

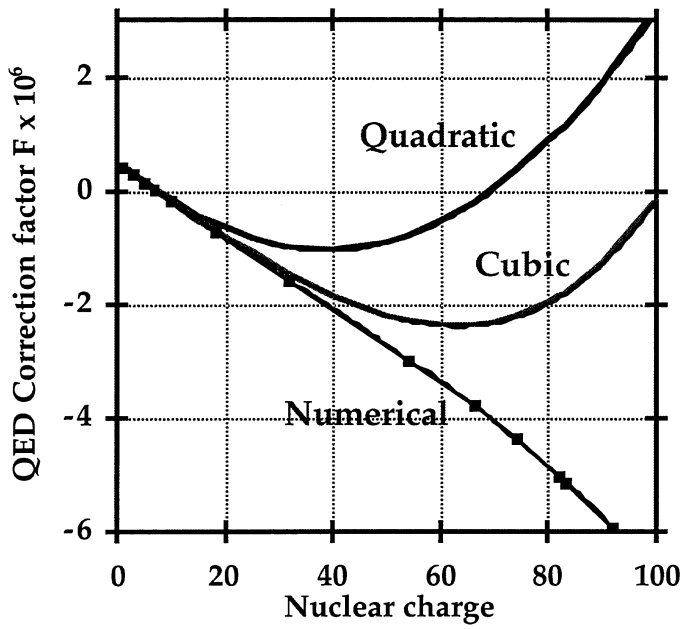

Fig. 7. Comparison between the results of the $Z\alpha$ expansion—to second and third order—with the all-order numerical result for the QED correction to the hyperfine structure of hydrogenlike systems.

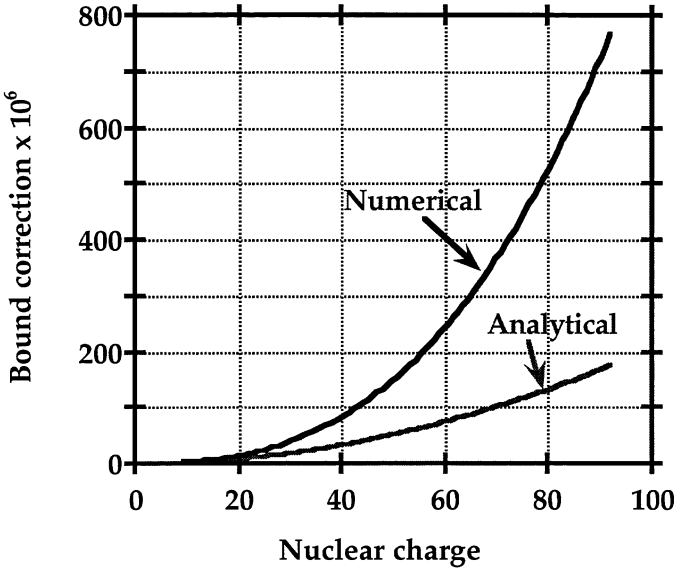

Fig. 8. Comparison between the results of the $Z\alpha$ expansion to second order and the all-order numerical results for the bound correction to the atomic g-factor for hydrogenlike systems.

4.2. *The Zeeman effect*

The Zeeman effect (g-factor) of singly charged ions has for some time been accurately studied in ion- trap experiments, and similar experiments on highly charged ions are now being prepared with an anticipated relative accuracy of $1{:}10^7$. The first experimental results have recently been reported for C^{+5} with an accuracy of $1{:}10^6$ [13].

For a free electron the g-factor is accurately known to be $2 \times 1.0011596\ldots$, where the dominating deviation from the Dirac value of 2 is the Schwinger correction, α/π. For a bound electron there are additional corrections,

$$g_{\text{bound}} = 2\left(1 + \frac{\alpha}{2\pi} + \cdots - \frac{(Z\alpha)^2}{3} + \cdots + \frac{\alpha(Z\alpha)^2}{12\pi} + \cdots\right).$$

Here, the third term is the leading relativistic correction, first evaluated by Breit [35], and the last term the leading radiative correction, calculated by Grotch and Hegstrom [36]. The radiative corrections have recently been calculated numerically to all orders in $Z\alpha$ by Blundell *et al.* [37] (self energy part) and Persson *et al.* [38] (self energy and vacuum polarization). The results of Persson *et al.* are displayed in Fig. 8 together with the analytical result of Grotch and Hegstrom. There it can be seen that the deviation between the analytical and numerical results become appreciable already for $Z > 20$.

5. Summary and Conclusions

In this review we have concentrated on a comparison between some recent experimental and theoretical results for heavy one- and few-electron systems, which can be used for testing QED at strong nuclear fields. For such systems, the conventional $Z\alpha$ expansion is no longer applicable, and numerical non-perturbative (all-order) techniques has to be employed.

The 1s binding energy of a number of heavy H-like ions have been measured with high accuracy, which makes it possible to extract the 1s Lamb shift. Good agreement is obtained with first-order QED calculations. The experimental accuracy is not yet good enough to test higher-order contributions, which, in addition, is expected to be largely masked by uncertainty in the nuclear effects.

Very accurate experimental data exist now for the 2s-2p transitions in several Li-like ions. Here the second-order Lamb-shift contributions, which are not yet fully calculated, are expected to be quite significant. Comparison between theoretical and experimental data might here constitute an important test of strong-field QED beyond the first order.

The binding energies of He-like ions in the groundstate have been compared experimentally with the corresponding H-like ions, yielding experimental values of the two-electron contribution to the binding energy of the He-like ions. Recent calculations give good agreement with experiments, although the experimental accuracy is not yet sufficient for testing the two-electron QED contributions. Accurate experimental data exist also for the separations between excited states of light and medium-heavy He-like ions. When more complete theoretical data will become available, interesting tests of strong-field QED can here be performed.

The hyperfine structure some heavy H-like ions has recently been measured with high accuracy. Recent calculations including QED effects give good agreement with the experimental result. However, the uncertainty of the nuclear magnetic moment as well as of the Bohr-Weisskopf often limits the value of the test. Very accurate measurements of the g-factor of highly charged H-like ions are now in preparation. The QED effects are here quite significant, and effects beyond leading order might be detected, also for quite relatively light or medium-heavy ions. The effect of the finite nuclear size is here extremely small, which makes these kind of experiments extremely interesting for QED test of tightly bound electrons.

Acknowledgments

I wish to acknowledge the long-lasting and productive collaboration with my coworkers in Göteborg, Sten Salomonson, Hans Persson and Per Sunnergren, as well as the fruitful collaboration with Walter Greiner and Stefan Schneider,

Frankfurt, Gerhard Soff, Günter Plunien and Thomas Beier, Dresden, Leonti Labzowsky and A. Mitrushenkov, St. Petersburg, and with the experimental Atomic Physics group at GSI, Darmstadt, under the leadership of Jürgen Kluge. The financial support of the Swedish Natural Research Council, the Knut & Alice Wallenberg Foundation and the von Humboldt Stiftung is acknowledged.

References

1. See, for instance, Schweber, S.S., "QED and the Men Who Made It: Dyson, Feynman, Schwinger and Tomanaga", Princeton University Press (1994), for an account of the early history of QED.
2. Uehling, E.A., Phys. Rev. **48**, 55 (1935).
3. Nafe, J.E., Nelson, E.B., and Rabi, I.I., Phys. Rev. **71**, 914 (1947); *ibid*. **73**, 718 (1948). See also, Ramsey, N.F., Adv. Quant. Chem. **30**, 5 (1998).
4. Breit, G., Phys. Rev. **71**, 984 (1947).
5. Kusch, P., and Foley, H.M., Phys. Rev. **72**, 1256 (1947); *ibid*. 74, 250 (1948).
6. Schwinger, J., Phys. Rev. **73**, 426 (1948); *ibid*. **76**, 790 (1949).
7. Lamb, W.E., and Retherford, R.C., Phys. Rev. **72**, 241 (1947).
8. See, for instance, Sapirstein, J., and Yennie, D.R., in "Quantum Electrodynamics," (edited by T. Kinoshita) (World Scientific, Singapore, 1990). See also Eides, M.I. and Karshenboim, S.G., and Shelyuto, V.A. Phys. Atomic Nuclei, **57**, 1240 (1994); Eides, M.I., and Shelyuto, V.A., Phys. Rev. A **52**, 954 (1995); Eides, M.I., and Grotch, H., Phys. Rev. A **52**, 3360 (1995); Kinoshita, T., and Nio, M., Phys. Rev. D **53**, 4909 (1996); Pachucki, K., Phys. Rev. Lett. **72**, 3154 (1996); Karshenboim, S.G., J. Exp. Theor. Phys. **82**, 403 (1996), J. Phys. B **29**, L29 (1996). See also Mohr, P., Adv. Quant. Chem. **30**, 77 (1998) for a recent update on the status of the least-squares adjustment of the fundamental constants.
9. a) Beyer, H.F. *et al*., Phys. Lett. A **184**, 435 (1994); Z. Phys. D **35**, 169 (1995). b) Stöhlker T. *et al*, (1998) (private communication).
10. a) Schweppe *et al*., J., Phys. Rev. Lett. **66**, 1434 (1991). b) Beiersdorfer, P., Osterheld, A.L., Scofield, J.H., Crespo Lopez-Urrutia, J.R., and Widman, K., Phys. Rev. Lett. **80**, 3022 (1998). c) Bosselman, Ph., Schartner, K.H., Livingstone, A.E., Folkman, F., and Mokler, P.H. (presented at the Bensheim conference Sept. 1998, unpublished).
11. Marrs, R.E., Elliott, S.R., and Stöhlker, T., Phys. Rev. A **52**, 35776 (1995).
12. Klaft, I. *et al*., Phys. Rev. Lett. **73**, 2425 (1994).
13. Hermanspahn, K. *et al*., Acta Physica Polonica B **27**, 357 (1996); Diederich, M. *et al*. (presented at the Bensheim conference Sept. 1998, unpublished).
14. Johnson, W.R., Blundell, S.A., and Sapirstein, J., Phys. Rev. A **40**, 5548, 5559 (1989).
15. Salomonson, S., and Öster, P., Phys. Rev. A **40**, 5548, 5559 (1989).
16. Mohr, P.J., Phys. Rev. **88**, 26 (1974); Phys. Rev. Lett. **34**, 1050 (1982); Mohr, P.J., and Soff, G., Phys. Rev. Lett. **70**, 158 (1993).
17. Wickman, E.H. and Kroll, H.M., Phys. Rev. **101**, 843 (1956).
18. Soff, G., and Mohr, P.J., Phys. Rev. A **38**, 5066 (1988).
19. Persson, H., Lindgren, I., Salomonson, S., and Sunnergren, P., Phys. Rev. A **48**, 2772 (1993).
20. Schneider, S.M., Greiner., and Soff, G., J. Phys. B **26**, L529 (1993). Plunien, G., Greiner, W., Soff, G., and Persson, H., Eur. Phys. J. D **1**, 177 (1998). Beier, T., Plunien, G., Greiner, W., and Soff, G., Z. Phys. B **30**, 2761 (1997). Lindgren, I., *et al*., J. Phys. B **26**, L503 (1993); Persson, H., *et al*., Phys. Rev. A **54**, 2805 (1996).
21. Mitrushenkov, A., Labzowsky, L., Lindgren, I., Persson H., and Salomonson, S., Phys. Lett. A **200**, 51 (1995). Lindgren, *et al*., J. Phys. B **26**, L503 (1993). Labzowsky, L.N., and Mitrushenkov, A., Phys. Rev. A **53**, 3029 (1995); Phys. Lett. A **198**, 333 (1995); Labzowsky, L.N., Goidenko, I.A., and Nefiodov, A.V., J. Phys. B **31**, L477 (1998). Mallampalli, S., and Sapirstein, J., Phys. Rev. A **57**, 1548 (1998); Phys. Rev. Lett. **24**, 5297 (1998). Lindgren, I., Persson, H., Salomonson, S., Sunnergren, P., Phys. Rev. A **57**, 1001 (1998).
22. a) Plunien, G., Müller, B., Greiner, W., and Soff, G, Phys. Rev. A **39**, 5428 (1989) and A **43**, 5853 (1991); Plunien, G. and Soff, G., Phys. Rev. A **53**, 4614 (1996). b) Artemyev, A.N., Shabaev, V.M., and Yerokhin, V.A., Phys. Rev. A **53**, 1884 (1995); Shabaev, V.M., *et al*., Phys. Rev. A **57**, 4235 (1998); Shabaev, V.M., Artemyev, A.N., Beier, T., and Soff, G., J. Phys. B **31**, L337 (1998).
23. Snyderman, N.J., Ann. Phys. A **44**, 1427 (1991); Blundell, S.A., and Snyderman, N.J., Phys. Rev. A **44**, 1427 (1991). S.A. Blundell, Phys. Rev. A **46**, 3762 (1992).
24. a) Persson, H., Lindgren, I., and Salomonson, S., Physica Scripta T **46**, 125 (1993). Lindgren, I., Persson, H., Salomonson, S., and Ynnerman, A., Phys. Rev. A **47**, R4555 (1993). b) Yerokhin, V.A., Artemyev, A.N., Beier, T., Shabaev, V.M., and Soff, G., J. Phys. B **31**, L691 (1998).
25. Quiney, H.M., and Grant, I.P., J. Phys. B **27**, L199 (1994).
26. Brown, G.E., and Ravenhall, D.G., Proc. Roy. Soc. London A **251**, 92 (1951).
27. Sucher, J., Phys. Rev. A **22**, 348 (1980).
28. Sucher, J., J. Phys. B **21**, L585 (1988). Lindgren, I., J. Phys. B **23**,1985 (1990).
29. a) Lindgren, I., Persson, H., Salomonson, S., and Labzowsky, L., Phys. Rev. A **51**, 1167 (1995); Persson, H., Salomonson, S., Sunnergren, P., and Lindgren, I., Phys. Rev. Lett. **76**, 204 (1996). b) Blundell, S., Mohr, P.J., Johnson, W.R., and Sapirstein, J., Phys. Rev. A **48**, 2615 (1993). c) Yerokhin, V.A., Artemyev, A.N., and Shabaev, V.M., Phys. Lett. A **234**, 361 (1997).
30. Persson, H., Schneider, S.M., Greiner, W., Soff, G., and Lindgren, I. Phys. Rev. Lett. **76**, 1433 (1996); P. Sunnergren, *et al.* Phys. Rev. A **57**, 1055 (1998).
31. Blundell, S.A., Cheng, K.T., and Sapirstein, J., Phys. Rev. A **55**, 1857 (1977).
32. Shabaev, V.M., Tomaselli, M., Kuhl, T., Artemyev, A.N., and Yerokhin, Y.A., Phys. Rev. A **56**, 252 (1997).
33. Pachucki, K., Phys. Rev. A **54**, 1994 (1996).
34. Karshenboim, S.G., Z. Phys. D **36**, 11 (1996).
35. Breit, G., Nature **122**, 649 (1928).
36. Grotch, H., Phys. Rev. Lett. **24**, 39 (1970); Grotch, H., and Hegstrom, R.A., Phys. Rev. A **4**, 59 (1971).
37. Blundell, S.A., Cheng, K.T., and Sapirstein, J., Phys. Rev. A **55**, 1857 (1997).
38. Persson, H., Salomonson, S., Sunnergren, P., and Lindgren, I., Phys. Rev. A **56**, R2499 (1997).